Optimal Design of Flat-Gain Wide-Band Fiber Raman Amplifiers

Victor E. Perlin and Herbert G. Winful, *Fellow, IEEE*

***Abstract*—We present a novel method for desiging multiwavelength pumped fiber Raman amplifiers with optimal gain-flatness and gain-bandwidth performance. We show that by solving the inverse amplifier design problem, relative gain flatness well below 1% can be achieved over bandwidths of up to 12 THz without any gain equalization devices. This constitutes a substantial improvement in gain flatness compared to the existing wide-band optical fiber amplifiers.**

***Index Terms*—Optical crosstalk, optical fiber amplifiers, optical fiber communication, optical fiber losses, optical fiber theory, Raman scattering.**

I. Introduction

BECAUSE the gain bandwidth of erbium-doped fiber amplifiers (EDFA) is much narrower than the low loss window of standard optical communication fibers, there is growing interest in wideband flat-gain optical fiber amplifiers (OFAs) to exploit more of the available fiber bandwidth and increase the capacity of wavelength division multiplexing (WDM) systems [1], [2]. Gain bandwidths in excess of 10 THz (approximately 80 nm) have been demonstrated using either hybrid fiber amplifiers [3]–[5] or fiber Raman amplifiers pumped at multiple wavelengths (MW-FRA) [6]–[10]. However, all of these amplifiers, especially those with larger bandwidths, have a serious drawback of poor gain flatness. Among the demonstrated OFAs with bandwidth exceeding 60 nm, the relative flatness lies within the 15%–30% range [4]–[9], which can be reduced to the 4%–10% range by the use of gain equalizers [10], [11].

In the case of Raman amplifiers with multiple pumps, the gain profile can be adjusted by appropriately choosing the relative positions and powers of the pump waves. In principle, this can allow for the design of amplifiers with any required gain spectra, e.g., the ones that would provide flat net gain. However, the corresponding inverse MW-FRA design problem has not been effectively solved (to the best of our knowledge). One of the main difficulties is that pump-to-pump and signal-to-signal Raman interactions make the system highly nonlinear, and even the direct problem of finding the gain profile, given the input pump distribution, becomes somewhat complicated and, numerically, rather time consuming for backward-pumped MW-FRA.

In this paper, we propose an efficient automatic method to solve the inverse amplifier design problem, which makes it possible to design multiwavelength pumped Raman amplifiers with gain flatness close to the optimum. Given amplifier specifications such as the signal level, required gain profile, and number of allowed pump channels, this method generates a combination of pump wavelengths and input powers that would result in the gain profile approximating the specified one as closely as possible. Optimizing the input pump spectrum by solving this inverse problem allows for a drastic improvement in the relative gain flatness compared to unoptimized MW-FRA designs [7]–[12].

Manuscript received April 18, 2001; revised October 25, 2001.

The authors are with the Department of Electrical Engineering and Computer Science, University of Michigan, Ann Arbor, MI 48109 USA (e-mail: vperlin@umich.edu).

Publisher Item Identifier S 0733-8724(02)00500-5.

II. Amplifier Model and Design Method

Wave propagation in the backward-pumped multipump Raman amplifier is characterized by a large number of effects [12], the most important of which, for the purposes of the present consideration, are pump-to-pump and pump-to-signal stimulated Raman scattering, and wavelength-dependent linear attenuation experienced by both pump and signal waves. In steady state, this system is described by the following set of coupled nonlinear equations:

$$\pm\frac{dP_k}{dz} = -\alpha_k P_k + \sum_{j=1}^{k-1} \frac{g_{\nu_j}(\nu_j-\nu_k)}{K_{\text{eff}}A_{\text{eff}}} P_j P_k - \sum_{j=k+1}^{m+n} \frac{\nu_k}{\nu_j}\frac{g_{\nu_k}(\nu_k-\nu_j)}{K_{\text{eff}}A_{\text{eff}}} P_j P_k, \quad k=1,2,\ldots,n+m. \quad (1)$$

Here, the frequencies are numerated in decreasing order ($\nu_i > \nu_j$ for $i < j$), indexes $k = 1, \ldots, n$ correspond to the backward-propagating pump waves (the minus sign on the left hand side) and indexes $k = n+1, \ldots, n+m$ correspond to the forward-propagating signal waves (plus sign on the left hand side). Here, the values P_i, ν_i, and α_i describe, respectively, the power, frequency, and attenuation coefficient for the ith wave, $i = 1, 2, \ldots, n+m$. The gain coefficients at pump frequency ν_i are given by $g_{\nu_i}(\Delta\nu) = g_R(\Delta\nu)\cdot\nu_i/\nu_0$, where $g_R(\Delta\nu)$ is the Raman gain spectrum measured at a reference pump frequency ν_0, A_{eff} is the effective area of the fiber, and K_{eff} is the polarization factor. Equation (1) is to be solved with the boundary conditions $P_k(L) = P_{k0}$ ($k = 1, 2, \ldots, n$) and $P_k(0) = P_{k0}$ ($k = n+1, \ldots, n+m$) for input pump and signal powers, respectively (L is the fiber length). The model described by (1) does not take into consideration spontaneous Raman scattering and Rayleigh backscattering, because these noise effects do not affect the amplifier gain profile.

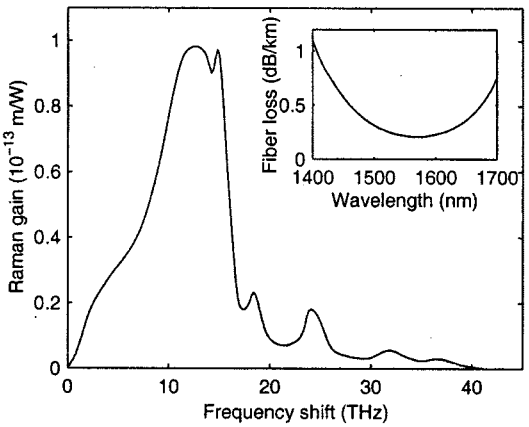

Fig. 1. Typical Raman gain spectrum $g_R(\Delta\nu)$ of a silica fiber at pump wavelength $\lambda_0 = 1$ μm. Inset shows the linear attenuation spectrum a silica fiber in the low loss window 1400–1700 nm.

The amplification factor for every signal channel $k = n+1, n+2, \ldots, n+m$ can be expressed in terms of the power integrals $I_j \equiv \int_0^L P_j(z)\,dz$, $j = 1, 2, \ldots, n+m$ as

$$\begin{aligned} G_k &\equiv \frac{P_k(L)}{P_k(0)} \\ &= \exp\left(-\alpha_k L + \sum_{j=n+1}^{n+m} g_{jk} I_j\right) \exp\left(\sum_{j=1}^{n} g_{jk} I_j\right) \\ &= G_{L,k} G_{G,k} \end{aligned} \tag{2}$$

where $g_{jk} = g_{\nu_j}(\nu_j - \nu_k)/K_{\text{eff}} A_{\text{eff}}$ for $\nu_j > \nu_k$ and $g_{jk} = -g_{\nu_k}(\nu_k - \nu_j)\nu_k/\nu_j K_{\text{eff}} A_{\text{eff}}$ for $\nu_j < \nu_k$. The first exponential term in (2), $G_{L,k}$, represents the effects of fiber attenuation and signal-to-signal Raman scattering (Raman tilt), whereas the second term, $G_{G,k}$, describes the ON–OFF or gross (pump-to-signal) Raman gain experienced by the channel k. Assuming the terms $G_{L,k}$ are known, the complex inverse problem finding the pump combination that yields the flattest net gain profile $G_k \simeq 1$ breaks into two simpler problems to be solved one after the other. The first problem is to find such a set of frequencies ν_j and constants I_j^* , so that the sum $\sum_{j=1}^n g_{jk} I_j^*$ is close to $\log G_{L,k}^{-1}$ for all of the frequencies ν_k within the specified gain band. The second problem is to find such a set of input pump powers P_{j0} for these frequencies, so that the solutions $P_j(z)$ of (1) with the initial conditions P_{j0} have the integrals I_j exactly equal to the optimal values I_j^*. We refer to the set of I_js as the integral pump spectrum.

The proposed design algorithm takes the Raman gain spectrum $g_R(\Delta\nu)$ and the attenuation spectrum $\alpha(\nu)$ of the fiber as the given *a priori* characteristics (see Fig. 1). Also, one should specify the amplifier length L, the input signal level P_{0s}, the wavelength range for signal and for pump waves, and the number of signal and pump channels m and n, respectively. In the first stage of the method, one out of all possible sets of n pairs (ν_j, I_j^*) is chosen to minimize the relative gain flatness parameter, defined as the difference (in decibels) between the maximal and the minimal gains $\log G_{G,k}$ normalized by their target values $\log G_{L,k}^{-1}$ as

$$F_{\text{rel}} \equiv \left[\left(\frac{\log G_{G,k}}{\log G_{L,k}^{-1}}\right)_{\max} - \left(\frac{\log G_{G,k}}{\log G_{L,k}^{-1}}\right)_{\min}\right] \cdot 100\%. \tag{3}$$

In order to find the best integral pumping spectrum $\{\nu_j, I_j^*\}_{j=1}^n$, we apply a genetic algorithm in a $2n$-dimensional object space [13]. Starting with a randomly chosen large set (population) of n-component pump spectra $\{\nu_j, I_j\}_{j=1}^n$, we iteratively apply the three evolution procedures (crossover, mutation, and natural selection) until the population fitness level stops improving, and the best (fittest) individual is chosen as the final pump spectrum. The fitness parameter (i.e., the parameter to be evolutionarily optimized) of an individual (spectrum $\{\nu_j, I_j\}_{j=1}^n$) is the corresponding relative gain flatness (3). On each iteration step (generation), a fixed number of the fittest individuals is chosen (natural selection); among them, couples are formed with their parameters mixed (crossover with discrete recombination) to create the next generation. Mutation is implemented by small random changes in one or more of $2n$ parameters of each individual. Notice that because the integral pump spectrum $\{\nu_j, I_j\}_{j=1}^n$ is being sought, the flatness computation does not require the time-consuming solution of (1), which enables the use of large enough population sizes. Consistency in the results shows that, for a reasonable number of pumps ($n < 20$), the optimal or nearly optimal integral pump spectrum can always be found.

At the second stage of the design procedure, we fix the optimal frequencies obtained in the first stage and search for the optimal input pump powers P_{j0}. To do this, we apply an iterative algorithm. Starting with some reasonable initial guess, which allocates relatively more power to the higher-frequency pump channels to compensate for pump-to-pump Raman interactions, we solve (1), compare the resulting pump power integrals I_j to the optimal values I_j^*, and adjust the input powers P_{j0} appropriately. The difficulty here is that, because of the highly nonlinear nature of the system (1), the increase in the input power P_{j0} for some pump channel j may not lead to an increase in the corresponding integral I_j. Nevertheless, we found it quite straightforward to adjust the iteration procedure so that it converges to the desired distribution. For any reasonable integral spectrum target $\{\nu_j, I_j^*\}_{j=1}^n$, we were able to obtain the input spectrum $\{\nu_j, P_{j0}\}_{j=1}^n$ so that the resulting integral spectrum $\{\nu_j, I_j\}_{j=1}^n$ matches the target with any given precision.

To conclude the description of this design algorithm, we have to resolve one remaining subtlety. Each iteration of the second stage requires the solution of (1), which could be efficiently implemented numerically by any marching method (e.g., Runge–Kutta), if the boundary conditions were all assigned at one point. However, in the case of backward pumping, the input pump powers are assigned at $z = L$ while the input signal powers are given at $z = 0$, which seriously complicates the numerical problem. We surmount this difficulty by assigning the boundary conditions for the signal powers at $z = L$ using

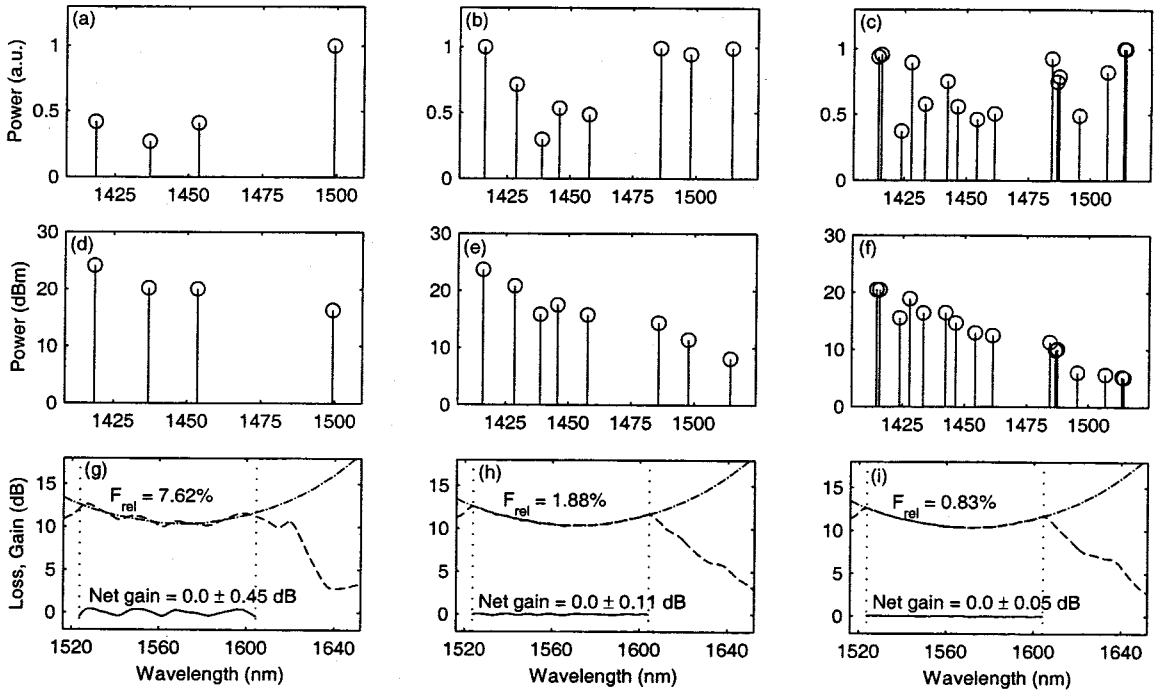

Fig. 2. Optimization results for 10 THz (83 nm) system with $n = 4, 8$, and 16 pump channels (left, central, and right columns, respectively). (a)–(c) optimal integral pump spectra. (d)–(f) optimal input pump spectra. (g)–(i) the corresponding gross gain (dashed lines), fiber attenuation (dash-dotted lines), and net gain profiles (solid lines). Vertical dotted lines indicate the band occupied by the signal channels.

(2) with the integral pump spectrum selected at the first stage of the method, $P_k(L) = P_k(0)G_{L,k}\exp(\sum_{j=1}^{n} g_{jk}I_j^*)$. This approach, which makes the proposed method fast and efficient, is valid only if the iterations converge to the target with high precision. Fortunately, this is always the case for the algorithm in question. In fact, this approach makes the numerical solution of the difficult inverse problem for backward-pumped MW-FRA (finding the input pump spectrum which would provide the specified gain profile) almost as fast as the numerical solution of the simpler direct problem (finding the gain, given the input pump spectrum).

It is important to notice that although the choice of pumps $\{\nu_j, P_{j0}\}_{j=1}^{n}$ depends on the terms $G_{L,k}$ in (2), these terms contain the signal power integrals I_j and, thus, depend on the pumping spectrum. Therefore, the MW-FRA design problem must be solved self-consistently. This difficulty can be overcome by iterating the procedure described here, starting with the signal power integrals computed in the absence of any pumping and updating them after each (outer) iteration step using the new values $\{\nu_j, P_{j0}\}_{j=1}^{n}$. Normally, these outer iterations converge very quickly (after three or four steps), because the effect of Raman tilt is relatively small, and the tilt does not change much with a moderate change in the pump powers. The typical run time for the whole optimization procedure $\sim 10^2$–10^3 s (for $n = 5$–20 pump waves, depending on the search depth in genetic algorithm) on a regular 1-GHz personal computer.

III. Numerical Example

We have applied the proposed method to design optimal flat-gain wide-bandwidth multiwavelength pumped Raman amplifiers operating in the 1500-nm region in standard single-mode silica fibers ($A_{\text{eff}} = 50\ \mu\text{m}^2$) with the Raman gain and attenuation spectra shown in Fig. 1. We fix the amplifier (or fiber span) length at a practical value of $L = 50$ km and the required net gain at $G = 0$ dB (the corresponding gross gain is ~10–13 dB for different channels). As an example, we consider a 10-THz WDM system pumped at $n = 4, 8$, or 16 wavelengths. There are $m = 100$ signal channels with 100-GHz spacing. We take the input signal level at -3 dBm/ch, and assume that the effect of Raman tilt is negligible, and the terms $G_{L,k}$ are simply the linear attenuation factors. The pump frequencies are chosen from the grid with 100-GHz spacing, which provides sufficient spectral resolution because the features of the Raman gain spectrum are substantially broader than 100 GHz.

The optimal pumping spectra and the corresponding Raman gain profiles are shown in Fig. 2. The ON–OFF (gross) Raman gain profile approaches the fiber attenuation profile resulting in flat net gain profile around 0 dB. The gain flatness improves dramatically with increase in the allowed number of pump channels and reaches the value of 0.83% for 16 pump channels. This corresponds to a signal power deviation of less than 0.05 dB from its initial value after propagation through a 50-km-long fiber span (for all of the channels). Fig. 3 shows the self-consistent evolution of the pump and signal channel powers (for the case $n = 16$) upon propagation through the amplifier. Shorter wavelength pump channels transfer power to the longer wavelength channels and decay more rapidly. This is compensated for by a substantial tilt in input pump power distribution (second row in Fig. 2). The total required pump power does not depend on the number of pump waves and is approximately 530 mW in this example.

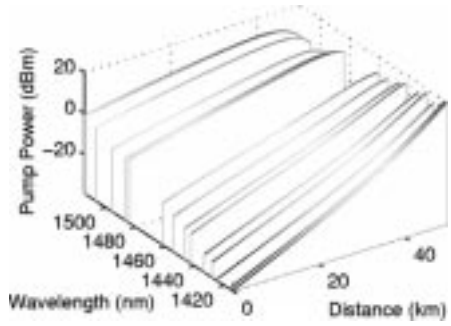

(a)

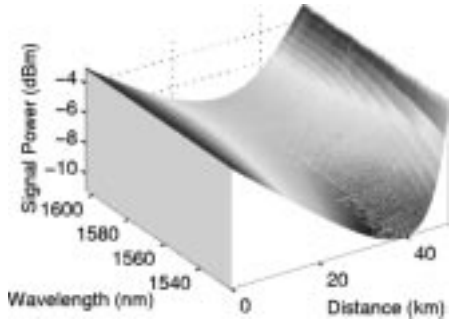

(b)

Fig. 3. Evolution of (a) pump and (b) signal powers upon propagation through the amplifier for $n = 16$. Data from the simulation of Fig. 2(c), (f), and (i).

IV. Discussion

The proposed method makes it possible to design multiwavelength pumped Raman amplifiers with the best possible (or very close to that) gain flatness within the specified constraints, such as the number of pump waves and the gain bandwidth. The capabilities of method in terms of achieving flat-gain wideband amplifiers are summarized in Fig. 4, which shows the best possible relative flatness [defined in (3)] as a function of the number of pump channels n for three different values of required gain bandwidth. Quite understandably, the achievable flatness degrades with the increase in the bandwidth and improves (faster than $1/n$) with the increase in the number of pump channels n. Also shown in Fig. 4 (open dots) are the flatness results for wideband Raman amplifiers without gain equalization, as reported in the literature (from [3]–[12]). Clearly, the relative flatness achievable by the proposed method is much better (with the other parameters kept equal) than that in the previously published results.[1] In fact, optimal design with a sufficiently large number of pump waves provides better flatness than that reported even for amplifiers with gain-equalizing filters, which can make the latter completely unnecessary. Obviously, this is a promising approach to gain-flattening, since no signal power is wasted for filtering, and, ultimately, the efficiency and noise performance of the optically amplified system are improved.

[1]Since the present paper was submitted for publication, at least three other papers devoted to the solution of the same problem (optimal design of MW-FRA) have been published [15]–[17]. However, the design method proposed in the present paper has some important advantages over the published methods. The iterative method of [15] requires a time-consuming solution of the system (1) on every iteration step, which limits the number of iterations and precludes it from finding optimal or close to that combinations. In [16], this system of equations is solved semianalytically under strong simplifying assumptions, but these assumptions would result in substantial errors when applied to a realistic system. Finally, the method presented in [17] is nonautomatic and, thus, impractical, especially for large number of pumps.

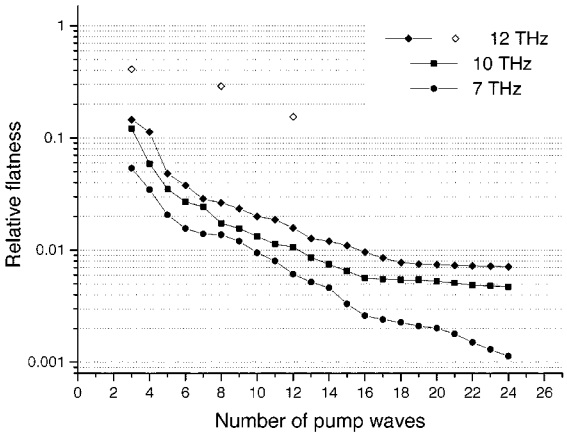

Fig. 4. Achievable relative gain flatness as a function of a number of pump channels for three values of gain bandwidth. Circles: 7 THz; squares: 10 THz; diamonds: 12 THz. Open diamonds correspond to the previously published results on multiwavelength pumped FRA with approximately 12-THz bandwidth (from [7], [9], and [12]).

As the example in Section III shows, the proposed method makes it possible to design MW-FRAs not only with flat gain but with any reasonably smooth gross gain profile to compensate for propagation effects such as wavelength-dependent fiber loss and signal-to-signal Raman scattering. The latter is particularly important for the long-haul transmission of a wideband signal [14]. It is important to notice that the achievable gain flatness depends on this profile; it improves for the concave and degrades for the convex on/off gain profiles (such as in Fig. 2). This is because the single-pump Raman gain spectrum (Fig. 1) is concave (except for a few small peaks), making it easier to generate concave composite profiles. The flatness results of Fig. 4 assume an intermediate case—flat gain profile—in order to be consistent with other publications.

In conclusion, we have proposed an efficient method of designing flat-net-gain wideband multiwavelength pumped fiber Raman amplifiers. The main feature of this method is that the inverse amplifier design problem is broken into two simpler inverse problems that are solved separately and, hence, efficiently. Compared to the previously published results, this method allows for substantial improvement, approaching the theoretical limits for gain flatness-bandwidth performance of fiber Raman amplifiers.

References

[1] S. Namiki and Y. Emori, "Recent advances in ultra-wideband Raman amplifiers," in *Proc. OFC 2000*, Baltimore, MD, 2000, FF1, pp. 98–99.
[2] H. Masuda, "Review of wideband hybrid amplifiers," in *Proc. OFC 2000*, Baltimore, MD, 2000, TuA1, pp. 2–4.
[3] J. Kani and M. Jinno, "Wideband and flat-gain optical amplification from 1460 to 1510 nm by serial combination of a thulium-doped fluoride fiber amplifier and fiber Raman amplifier," *Electron. Lett.*, vol. 35, pp. 1004–1006, June 10, 1999.
[4] S. Kawai, H. Masuda, K.-I. Suzuki, and K. Aida, "Wide-bandwidth and long-distance WDM transmission using highly gain-flattened hybrid amplifier," *IEEE Photon. Technol. Lett.*, vol. 11, pp. 886–888, July 1999.

[5] D. Bayart, P. Baniel, A. Bergonzo, J.-Y. Boniort, P. Bousselet, L. Garca, D. Hamoir, F. Lepringard, A. Le Sauze, P. Nouchi, F Roy, and P. Sillard, "Broadband optical fiber amplification over 17.7 THz range," *Electron. Lett.*, vol. 36, pp. 1569–1671, Aug. 31, 2000.

[6] H. Kidorf, "Recent advances in Raman amplification and applications," in *Proc. CLEO 2001*, Baltimore, MD, 2001, CTuJ3.

[7] Y. Emori, K. Tanaka, and S. Namiki, "100 nm bandwidth flat-gain Raman amplifiers pumped and gain-equalized by 12-wavelength-channel WDM laser diode unit," *Electron. Lett.*, vol. 35, pp. 1355–1356, Aug. 1999.

[8] S. A. E. Lewis, S. V. Chernikov, and J. R. Taylor, "Gain and saturation characteristics of dual-wavelength-pumped silica-fiber Raman amplifiers," *Electron. Lett.*, vol. 35, pp. 1178–1179, July 1999.

[9] ——, "Triple wavelength pumped silica-fiber Raman amplifiers with 114-nm bandwidth," *Electron. Lett.*, vol. 35, pp. 1761–1762, Sept. 1999.

[10] F. Koch, S. A. E. Lewis, S. V. Chernikov, J. R. Taylor, V. Grubsky, and D. S. Starodubov, "Broadband gain flattened Raman amplifier to extend operation in the third telecommunication window," in *Proc. OFC 2000*, Baltimore, MD, 2000, FF3, pp. 103–105.

[11] H. Masuda and S. Kawai, "Wide-band and gain flattened hybrid fiber amplifier consisting of an EDFA and a multiwavelength pumped Raman amplifier," *IEEE Photon. Technol. Lett.*, vol. 11, pp. 647–649, June 1999.

[12] H. Kidorf, K. Rottwitt, M. Nissov, M. Ma, and E. Rabarijaona, "Pump interactions in a 100-nm bandwidth Raman amplifier," *IEEE Photon. Technol. Lett.*, vol. 11, pp. 530–532, May 1999.

[13] Z. Michalewicz, *Genetic Algorithms + Data Structures = Evolution Programs*. New York: Springer-Verlag, 1992.

[14] S. Bigo, S. Gauchard, A. Bertaina, and J.-P. Hamaide, "Experimental investigation of stimulated Raman scattering limitation on WDM transmission over various types of fiber infrastructures," *IEEE Photon. Technol. Lett.*, vol. 11, pp. 671–673, June 1999.

[15] M. Yan, J. Chen, W. Jiang, J. Li, J. Chen, and X. Li, "Automatic design scheme for optical-fiber Raman amplifiers backward-pumped with multiple laser diode pumps," *IEEE Photon. Technol. Lett.*, vol. 13, pp. 948–950, 2001.

[16] X. Zhou, C. Lu, P. Shum, and T. H. Cheng, "A simplified model and optimal design of a multiwavelength backward-pumped Raman amplifier," *IEEE Photon. Technol. Lett.*, vol. 13, pp. 945–947, Sept. 2001.

[17] Y. Emori and S. Namiki, "Broadband Raman amplifier for WDM," *IEICE Trans. Electron.*, vol. E84-0C, pp. 593–597, Sept. 2001.

Victor E. Perlin, photograph and biography not available at the time of publication.

Herbert G. Winful (S'73–M'76–SM'86–F'94), photograph and biography not available at the time of publication.